Journal of Medicinal Chemistry Article

J. Med. Chem. **2010,** *53,* 5439–5448 **5439**
DOI: 10.1021/jm901808w

A Type-II Kinase Inhibitor Capable of Inhibiting the T315I "Gatekeeper" Mutant of Bcr-Abl

Hwan Geun Choi,[†,∥] Pingda Ren,[‡] Francisco Adrian,[‡] Fangxian Sun,[‡] Hyun Soo Lee,[‡] Xia Wang,[‡] Qiang Ding,[‡] Guobao Zhang,[‡] Yongping Xie,[‡] Jianming Zhang,[†] Yi Liu,[‡] Tove Tuntland,[‡] Markus Warmuth,[‡] Paul W. Manley,[§] Jürgen Mestan,[§] Nathanael S. Gray,*[,†] and Taebo Sim*[,‡,∥]

[†]*Dana Farber Cancer Institute, Harvard Medical School, Department of Cancer Biology and Department of Biological Chemistry and Molecular Pharmacology, 250 Longwood Avenue, Seeley G. Mudd Building 628A, Boston, Massachusetts 02115,* [‡]*Genomics Institute of the Novartis Research Foundation, Department of Chemistry, 10675 John Jay Hopkins Drive, San Diego, California 92121,* [§]*Novartis Institutes for Biomedical Research, CH-4056 Basel, Switzerland, and* [∥]*Life Sciences Research Division, Korea Institute of Science and Technology, 39-1 Hawolgok-dong, Seongbuk-gu, Seoul 136-791, Korea*

Received December 8, 2009

The second generation of Bcr-Abl inhibitors nilotinib, dasatinib, and bosutinib developed to override imatinib resistance are not active against the T315I "gatekeeper" mutation. Here we describe a type-II T315I inhibitor **2** (**GNF-7**), based upon a 3,4-dihydropyrimido[4,5-*d*]pyrimidin-2(1*H*)-one scaffold which is capable of potently inhibiting wild-type and T315I Bcr-Abl as well as other clinically relevant Bcr-Abl mutants such as G250E, Q252H, Y253H, E255K, E255V, F317L, and M351T in biochemical and cellular assays. In addition, compound **2** displayed significant in vivo efficacy against T315I-Bcr-Abl without appreciable toxicity in a bioluminescent xenograft mouse model using a transformed T315I-Bcr-Abl-Ba/F3 cell line that has a stable luciferase expression. Compound **2** is among the first type-II inhibitors capable of inhibiting T315I to be described and will serve as a valuable lead to design the third generation Bcr-Abl kinase inhibitors.

Introduction

The successful development of the Bcr-Abl[a] inhibitor imatinib for the treatment of chronic myelogenous leukemia (CML) has provided the paradigm for the development of a host of other small molecule inhibitors targeting kinases whose activity becomes deregulated in cancer. One major problem facing the development of selective protein kinase inhibitors is the emergence of drug resistance caused by mutations in the kinase domain. Extensive in vitro and clinical work has elucidated a large number of mutations that confer resistance to imatinib either by directly influencing the drug binding site or by disfavoring the conformational rearrangements required for imatinib to bind. Several second generation Bcr-Abl inhibitors have been developed including nilotinib (AMN107),[1] bosutinib (SKI-606),[2] and dasatinib (BMS-354825)[3] that are capable of inhibiting most of the known Bcr-Abl mutants with the exception of the so-called "gatekeeper" mutation T315I.[4]

Several small molecules capable of inhibiting the T315I mutant in biochemical and cellular assays have been reported.

*To whom correspondence should be addressed. For T.S.: phone, 82-2-958-6437; fax, 82-2-958-5189; E-mail, tbsim@kist.re.kr. For N.S.G.: phone, 1-617-582-8590; fax, 1-617-582-8615; E-mail, nathanael_gray@dfci.harvard.edu.

[a] Abbreviations: Axl, Axl receptor tyrosine kinase; ATP, adenosine triphosphate; AUC, area under the concentration time curve; Bcr-Abl, breakpoint cluster region abelson tyrosine kinase; BMX, BMX non-receptor tyrosine kinase; CaMKIV, calcium/calmodulin-dependent protein kinase type IV; CDK, cyclin-dependent kinases; CHK2, checkpoint homologue 2; CK2, casein kinase II; C-Kit, receptor tyrosine kinase for the cytokine stem cell factor; CLs, clearance; Clast, last measured concentration; C_{max}, maximum concentration observed; *m*-CPBA, *meta*-chloroperoxybenzoic acid; C-Raf, V-raf-1 murine leukemia viral oncogene homologue 1; Csk, C-terminal Src kinase; DCM, dichloromethane; DDR, discoidin domain receptor tyrosine kinase; DFG, aspartic acid phenylalanine glycine; DIEA, *N*,*N*-diisopropylethylamine; DMF, *N*,*N*-dimethylformamide; DMSO, dimethyl sulfoxide; EGFR, epidermal growth factor receptor; *F*, bioavailability; Fes, feline sarcoma oncogene; FGFR1, fibroblast growth factor receptor 1; FGFR3, fibroblast growth factor receptor 3; FLT3, FMS-like tyrosine kinase 3; FLT3-ITD, FLT3 internal tandem duplication; FT-NMR, Fourier transform nuclear magnetic resonance; GSK3β, glycogen synthase kinase 3β; HATU, 2-(1*H*-7-azabenzotriazol-1-yl)-1,1,3,3-tetramethyl uronium hexafluorophosphate; IC_{50}, half-maximal inhibitory concentration; IKKα, IκB (inhibitor of κ B) kinase α; IKKβ, IκB kinase β; IR, insulin receptor; Jak1,Janus kinase 1; JNK, c-Jun N-terminal kinase; LCK, lymphocyte-specific protein tyrosine kinase; Lyn, v-yes-1 Yamaguchi sarcoma viral related oncogene homologue; MAPK1, mitogen-activated protein kinase 1; MAPKAP-K2, MAP kinase-activated protein kinase 2; MEK1, MAP kinase kinase 1; MKK4, MAP kinase kinase 4; MKK6, MAP kinase kinase 6; NPM-ALK, nucleophosmin-anaplastic lymphoma kinase; p70S6K, p70 S6 kinase; P-loop, phosphate-binding loop; PAK2, p21 activated kinase 2; Pd/C, palladium on carbon or palladium on charcoal; PDGFR, platelet derived growth factor receptor; PDK1, phosphoinositide-dependent kinase-1; PEG, polyethylene glycol; PK, pharmacokinetics; PKBα, AKT family protein kinase; PKCα, protein kinase C α; PKD2, protein kinase D2; PO, peroral (orally); PP1, 4-amino-5-(4-methylphenyl)-7-(*t*-butyl)pyrazolo[3,4-*d*]pyrimidine; QD, quaque die/once a day; R_f, retention factor; ROCK-II, Rho-associated coiled-coil containing protein kinase 2; Rsk1, p90 ribosomal S6 kinase 1; SAPK2, stress activated protein kinase 2; SAPK3, stress activated protein kinase 3; SGK, serum/glucocorticoid regulated kinase; SCID, severe combined immunodeficiency; Src, transforming sarcoma inducing gene of Rous sarcoma virus; Syk, spleen tyrosine kinase; *T*/*C*, treated versus control (untreated); $T_{1/2}$, elimination half-life; TFA, trifluoroacetic acid; THF, tetrahydrofuran; T_{last}, time of last measured; T_{max}, time to maximum concentration; TPR-Met, translocated promoter region mesenchymal-epithelial transition factor; TrkC, neurotrophic tyrosine kinase receptor type 3; TrkB, neurotrophic tyrosine kinase receptor type 2; VEGFR2, vascular endothelial growth factor receptor 2; Vss, volume in steady state; UV, ultraviolet; ZAP-70, ζ-chain-associated protein kinase 70.

Published on Web 07/06/2010

(*E*)-*N*-Benzyl-2-cyano-3-(3,4-dihydroxyphenyl)acrylamide (AG-490),[5] an inhibitor of Jak2 which is a kinase implicated in signal transduction downstream of Bcr-Abl, was shown to induce apoptosis in Ba/F3-Bcr-Abl-T315I cell line.[6] 2-Cyclopentyl-*N*-(4-(dipropylphosphoryl)phenyl)-9-ethyl-9*H*-purin-6-amine (AP23846),[7,8] originally developed as a Src kinase inhibitor, inhibits T315I Bcr-Abl dependent cellular proliferation (IC_{50} of 297 nM) but also inhibits parental Ba/F3 cell lines, suggesting it possesses additional intracellular targets. *N*-(4-(4-(5-Methyl-1*H*-pyrazol-3-ylamino)-6-(4-methylpiperazin-1-yl)-pyrimidin-2-ylthio)phenyl)cyclopropanecarboxamide (VX-680, MK-0457),[9] originally developed as an aurora kinase inhibitor, exhibits potent enzymatic inhibition of T315I-Abl (IC_{50} of 30 nM) but only modestly inhibited cellular autophosphorylation (IC_{50} of ca. 5 μM) of Ba/F3 transformed with T315I Bcr-Abl.[10] Another Aurora kinase inhibitor, danusertib (PHA-739358),[11] currently being investigated in a phase II clinical trial for patients with relapsed chronic myelogeneous leukemia, exhibited potent inhibition of T315I-Abl enzyme (IC_{50} of 5 nM). Crystallographic analysis of danusertib in complex with T315I-Abl reveals[12] that the isoleucine side chain of T315I mutant does not cause a steric clash with danusertib in contrast to imatinib. (*E*)-4-(2-(2-(6-(4-(2-Hydroxyethyl)piperazin-1-yl)-2-methylpyrimidin-4-ylamino)thiazol-5-yl)vinyl)-phenol (TG101113),[13] a thiazole-based inhibitor, also exhibited good potency (IC_{50} of 66 nM) against T315I mutant enzyme. Another reported class of Bcr-Abl inhibitor is exemplified by (*R*,*E*)-2-(5-methoxy-2-((2,4,6-trimethoxystyrylsulfonyl)methyl)phenylamino)propanoic acid (ON012380),[14] which is claimed to be a non-ATP-competitive Bcr-Abl inhibitor, potently inhibits imatinib-resistant Bcr-Abl mutants such as T315I in cellular and biochemical assays, with IC_{50} values below 10 nM. This compound appears to target substrate binding site of Abl kinase domain, but numerous other cellular kinases are inhibited by this compound. It should be noted that most T315I inhibitors disclosed to date are categorized as type-I kinase inhibitors which bind exclusively to the ATP binding site of kinase. Recently, a few compounds from the type-II class that recognize the "DFG-out" conformation have been reported to inhibit T315I. These include (*E*)-3-(2-(6-(cyclopropylamino)-9*H*-purin-9-yl)vinyl)-4-methyl-*N*-(3-(4-methyl-1*H*-imidazol-1-yl)-5-(trifluoromethyl)-phenyl)benzamide (AP24163)[15] and DSA series compounds.[16] This 9-(arenethenyl)purine analogue exhibited modest potency (IC_{50} of 400 nM) against T315I in biochemical and cellular assays and *N*-(3-(3-(4-(4-methoxyphenylamino)-1,3,5-triazin-2-yl)pyridin-2-ylamino)-4-methylphenyl)-4-((4-methylpiperazin-1-yl)methyl)benzamide (DSA8) showed great potency (IC_{50} of 33 nM) on T315I enzyme along with moderate antiproliferative activity (IC_{50} of 500 nM) evaluated using T315I Bcr-Abl transformed Ba/F3 cells. A cocrystal structure with wild-type and gatekeeper mutant of Src with a PP1-based type-II inhibitor revealed how the inhibitor could leave ample space for an enlarged gatekeeper residue.[17] Most recently, it has been disclosed that 3-(imidazo[1,2-*b*]pyridazin-3-ylethynyl)-4-methyl-*N*-(4-((4-methylpiperazin-1-yl)methyl)-3-(trifluoromethyl)phenyl)benzamide (AP24534), an imidazo[1,2-*b*]pyridazine-based multitargeted kinase inhibitor, possesses potent inhibitory activity against T315I in cellular and in vivo models.[18]

Results and Discussion

Here we describe a type-II T315I inhibitor (Figure 1), based upon a 3,4-dihydropyrimido[4,5-*d*]pyrimidin-2(1*H*)-one scaffold

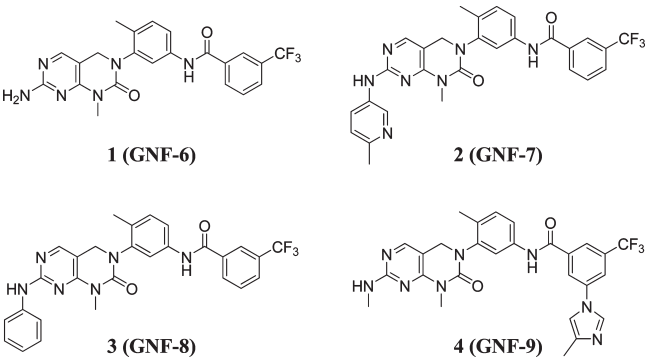

Figure 1. 3,4-Dihydropyrimido[4,5-*d*]pyrimidin-2(1*H*)-one scaffold for type-II T315I inhibitors.

which occupies the ATP binding cleft as well as an immediately adjacent hydrophobic pocket of Abl kinase domain. A representative member of this class, **1** (**GNF-6**)[19] was crystallized with Abl and shown to bind in the type-II conformation. The pyrimidopyrimidinone inhibitor described here, **2**, is capable of inhibiting wild-type and T315I Bcr-Abl activity in biochemical and cellular assays and also inhibits other clinically relevant Bcr-Abl mutants such as G250E, Q252H, Y253H, E255K, E255 V, F317L, and M351T. We also demonstrate that **2** is capable of inhibiting T315I-Bcr-Abl dependent tumor growth in a murine model of CML.[1]

Chemistry. The synthesis of compounds **1**−**4** commenced from commercially available ethyl 4-chloro-2-(methylthio)-pyrimidine-5-carboxylate. Scheme 1 shows an efficient synthetic route for making **1**−**3**, all of which bear 3-(trifluoromethyl)-benzamide moeity in the "tail region". The quantitative displacement of chloride group on compound **5** with methylamine proceeded readily at low reaction temperatures. The reduction of ester compound **6** with $LiAlH_4$ followed by oxidation using MnO_2 afforded the corresponding aldehyde compound **8** in high yields. One-pot reductive amination reaction using $Na(CN)BH_3$ proceeded smoothly to provide diamine derivative **10**, which was subsequently subjected to cyclic urea formation with triphosgene to give compound **11**. An elevated reaction temperature was required to complete this cyclic urea formation. Exposure of the sulfide group of compound **11** to *m*-CPBA resulted in the corresponding sulfone compound **12**, which could be transformed into the desired amine compounds. Ammonia and aniline were readily reacted with this sulfone compound **12** under simple thermal amination conditions to furnish **1** and **3**, respectively, in good (> 70%) yields. The synthesis of **2** required the presence of trifluoroacetic acid and elevated reaction temperature to catalyze the coupling of 6-methylpyridin-3-amine and sulfone compound **12**.

Compound **4** contains 4-methylimidazole group on the 3-(trifluoromethyl)benzamide "tail" in common with nilotinib. Scheme 2 describes an effective synthetic route which allows facile modification of 3-(trifluoromethyl)benzamide "tail" as is exemplified by the synthesis of **4**. Amide coupling reaction of aniline derivative **16** and carboxylic acid derivative **17** derived from 3-fluoro-5-(trifluoromethyl)benzonitrile was effected using HATU and DIEA in 89% yield.

Design Rationale for a Type-II T315I Bcr-Abl Inhibitor. An examination of the cocrystal structures of imatinib,[20] nilotinib,[1] and dasatinib[21] with Abl demonstrate that all three inhibitors form a critical hydrogen bond with the side-chain hydroxyl group of T315I and would also require a significant

Scheme 1[a]

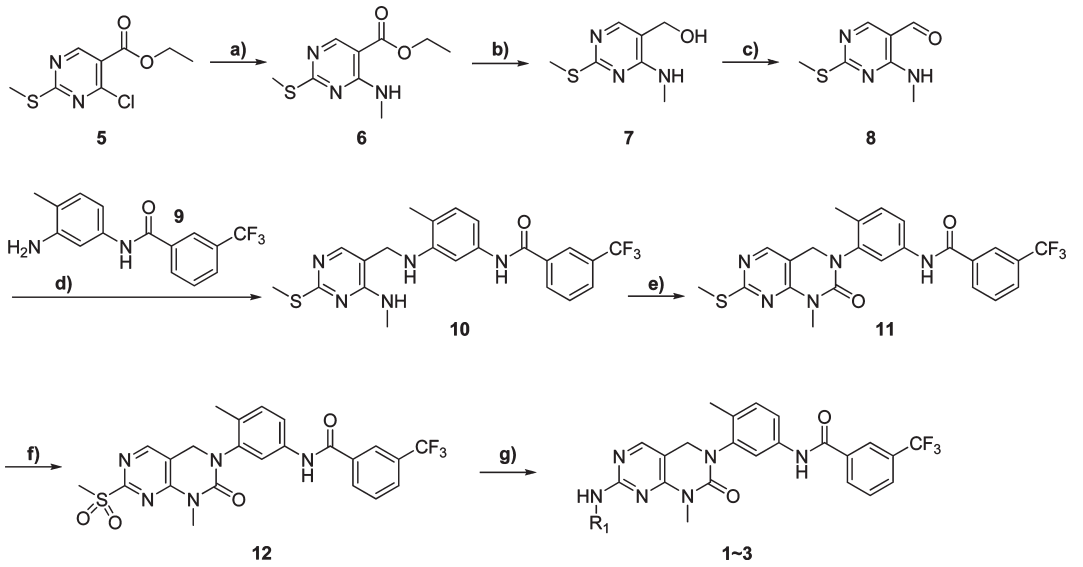

[a] Reagents and conditions: (a) methylamine, THF, 0 °C; (b) $LiAlH_4$, THF, 0 °C; (c) MnO_2, DCM; (d) $Na(CN)BH_3$, AcOH, MeOH; (e) triphosgene, DIEA, THF, 0 °C; (f) *m*-CPBA, DCM, 0 °C; (g) NH_3 in 2-propanol or aniline, 1,4-dioxane, 120 °C.

Scheme 2[a]

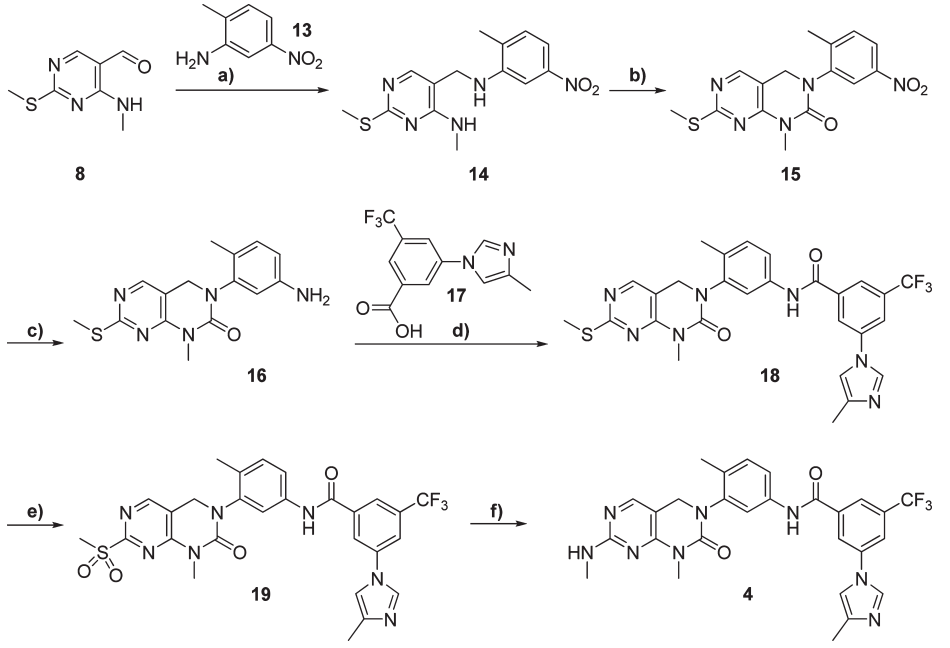

[a] Reagents and conditions: (a) $Na(CN)BH_3$, AcOH, MeOH; (b) triphosgene, DIEA, THF; (c) Pd/C, H_2, MeOH; (d) HATU, DIEA, DMF; (e) *m*-CPBA, DCM, 0 °C; (f) methylamine in THF, 1,4-dioxane, 120 °C.

rearrangement of their binding conformation to accommodate a larger residue at the gatekeeper position. Mutation of this gatekeeper position appears to be a general theme for resistance to kinase inhibitors.[22−25] Pyridopyrimidinones such as **20** (PD173955, 6-(2,6-dichlorophenyl)-8-methyl-2-[(3-methylsulfanylphenyl)amino]pyrido[6,5-*d*]pyrimidin-7-one) were originally developed as inhibitors of Src kinase[26] and receptor tyrosine kinase inhibitors such a EGFR, FGFR, PDGFR, and c-Kit[27] and were only later demonstrated to possess potent cellular and enzymatic activity on wild-type and mutant forms of Bcr-Abl.[28] Co-crystal structures of **20** with Abl (PDB: 1m52) demonstrate that this compound binds to the ATP-binding site with the kinase otherwise assuming a conformation normally utilized to bind ATP (type-I binding).[20] Interestingly, **20** exhibits approximately 30-fold more potent cellular activity against Bcr-Abl relative to imatinib, presumably as a consequence of possessing a much higher affinity to the ATP-binding pocket.[28b] In contrast, imatinib only exhibits cellular activity against Bcr-Abl and some receptor kinases, such as KIT, PDGFR, and DDR1/2, but is known not to inhibit the cellular activity of any Src-family kinases. The crystal structure of imatinib bound to the kinase domain of c-Abl[20] demonstrated that the compound binds to a conformation of the kinase where the activation loop is in a so-called "inactive" conformation (type-II binding). This binding conformation allows the piperazine-benzamide "tail" moiety of

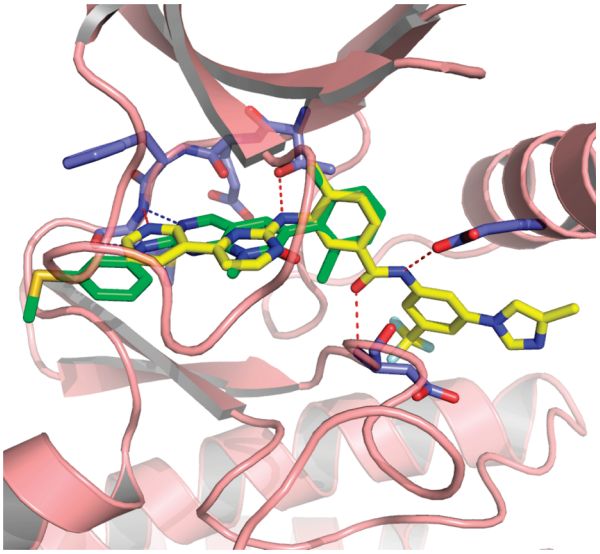

Figure 2. Superimposed structure of **20** (green sticks) bound to Abl (pink ribbon PDB: 1m52) and nilotinib (yellow sticks) bound to Abl (PDB: 3cs9). Hydrogen bonds are indicated by red hatched lines to key amino acids (blue sticks).

imatinib to access an additional hydrophobic pocket directly adjacent to the ATP binding site. By superimposing the bound conformation of **20** and nilotinib as depicted in Figure 2, it is clear that additional functionality can be appended to the dichlorophenyl ring of **20** to access this adjacent hydrophobic pocket to create a new "hybrid" structure.[19,29] We hypothesized that the resulting hybrid compound might be able to inhibit the T315I mutation due to enhanced affinity both to the hinge-binding region and to the hydrophobic back-pocket in addition to not forming a hydrogen bond to the gatekeeper position.

In Vitro Potency. To assess the cellular activity of the compounds, we tested them against wild-type and mutant Bcr-Abl transformed Ba/F3 cells. Wild-type Ba/F3 cells require the presence of interlukin-3 (IL-3) for growth and survival, but Ba/F3 cells transformed by oncogenic kinase such as Bcr-Abl becomes capable of growing in the absence of IL-3, which provides a robust and commonly used assay for selective kinase inhibition.[30] The first hybrid compound we made, compound **1**, exhibited an IC_{50} of less than 5 nM on wild-type Bcr-Abl and an IC_{50} of 303 nM on T315I while exhibiting non-specific inhibition of untransformed Ba/F3 cells with an IC_{50} of 1.7 μM (Table 1). Compound **1** also effectively inhibited cellular kinase autophosphorylation of T315I-Bcr-Abl-Ba/F3 with an IC_{50} of 243 nM, further demonstrating that the antiproliferative activity against this mutant correlates with direct inhibition of the T315I-Abl enzyme. A cocrystal structure[19] of **1** with Abl revealed that the compound bound to a conformation that was virtually indistinguishable from that used by imatinib, which clearly validates the design strategy.[31] We next evaluated how altering the structure in the hinge binding region and hydrophobic back pocket might change the potency of cellular inhibition. We replaced the amino-pyrimidine hinge binding motif of **1** with the phenylaminopyrimidine motif, which is known to form a stronger interaction with the kinase hinge residues as shown for **2** and **3**. These modifications improved absolute cellular potency against T315I as well as increase the ratio for selectivity relative to untransformed Ba/F3 cells. In addition, these modifications resulted in improved inhibitory potency on

Table 1. In Vitro Potency Profiling for 3,4-Dihydropyrimido[4,5-*d*]pyrimidin-2(1*H*)-one on Bcr-Abl

	compd code			
	1	**2**	**3**	**4**
Antiproliferative Activity on Native or Bcr-Abl Transformed Ba/F3 Cells (IC_{50}, nM)				
native Ba/F3	1799	1370	2690	1785
wtBcr-Abl	< 5	< 5	< 5	< 5
G250E	294	< 5	12	< 5
Q252H	< 5	< 5	19	16
Y253H	< 5	< 5	< 5	15
E255K	< 5	< 5	22	13
E255 V	< 5	< 5	27	30
T315I	**303 (243[a])**	**11**	**21**	**43**
F317L	< 5	< 5	6	< 5
M351T	< 5	< 5	< 5	< 5
Enzymatic Activity (IC_{50}, nM)				
c-Abl	< 5	133	135	< 5
G250E	ND	136	206	720
E255 V	< 5	122	< 5	< 5
T315I	**1567**	**61**	**130**	**< 5**
M351T	< 5	< 5	< 5	ND

[a] Inhibitory potency (IC_{50}, nM) against cellular kinase autophosphorylation (Elisa), ND means not determined.

Table 2. The Growth Inhibitory Potency (IC_{50}, μM) of **2**

cell line	IC_{50}, μM
TPR-Met-Ba/F3	3.401
NPM-ALK-Ba/F3	1.466
JAK1-Ba/F3	0.044
JAK2-Ba/F3	0.127
JAK2-V617F−Ba/F3	0.050
JAK3-Ba/F3	2.018
FGFR3-Ba/F3	0.009
Flt3-Ba/F3	0.359
Flt3-ITD-Ba/F3	0.012
PDGFR-Ba/F3	0.011
TrkC-Ba/F3	0.008
Colo205	0.005
SW620	0.001
U87	5.956
HEK293T	> 10

T315I enzyme as well as against T315I cellular autophosphorylation. We next incorporated a 3-methylimidazole by analogy to nilotinib, and the resulting compound **4** also demonstrated excellent activity against wild-type and mutant Bcr-Abl (Table 1). In particular, this methylimidazole of **4** significantly contributes to excellent potency (IC_{50} of < 5 nM) of **4** against T315I enzyme.

Compound **2** displayed excellent growth inhibitory activity against human colon cancer cells (Colo205 and SW620), while a noncancer cell line, HEK293T, was not particularly sensitive to inhibition by **2** as described in Table 2. As discussed below, the large number of kinases inhibited by **2** would suggest that additional profiling of this inhibitor against a larger panel of human cancer cell lines[32] would potentially reveal additional utility for this inhibitor.

Kinase Selectivity of 2. We next investigated the kinase selectivity of **2** against a panel of 41 recombinant kinase enzymes and on a panel of Ba/F3 cell lines transformed with a diverse set of tyrosine kinases as summarized in Tables 2 and 3. This analysis revealed that **2** is capable of potently inhibiting a large number of tyrosine and serine/threonine kinases. Despite its broad kinase selectivity profile, compound

Table 3. Kinase Selectivity Profile of **2**: Enzymatic Activity (% Inhibition) of **2** at 10 μM

kinase	% inhibition at 10 μM	kinase	% inhibition at 10 μM
Aurora-A(h)	31	MAPKAP-K2(h)	0
Axl(h)	69	MEK1(h)	58
Bmx(h)	98	MKK4(m)	98
c-RAF(h)	100	MKK6(h)	100
CaMKIV(h)	0	p70S6K(h)	92
CDK1/cyclinB(h)	3	PAK2(h)	45
CHK2(h)	12	PDGFRα(h)	62
CK2(h)	6	PDK1(h)	0
CSK(h)	100	PKBα(h)	7
Fes(h)	98	PKCα(h)-His	51
FGFR3(h)	100	PKCθ(h)	22
Flt3(h)	69	PKD2(h)	77
GSK3ss(h)	59	ROCK-II(h)	2
IKKα(h)	69	Rsk1(h)	95
IKKss(h)	49	SAPK2a(h)	95
IR(h)	89	SAPK2b(h)	98
JNK1α1(h)	97	SAPK3(h)	35
JNK2α2(h)	99	SGK(h)	0
Lck(h)	99	Syk(h)	98
MAPK1(h)	68	TrkB(h)	100
		ZAP-70(h)	6

Table 4. Pharmacokinetic Properties of **2** on Balb/C Mouse

formulation	PEG300 (100%), solution	PEG300/water 1:1, solution
dosing	5 mpk, intravenous	20 mpk, peroral
CLs (mL/min/kg)	8.6	
Vss (L/kg)	1.12	
AUC (h·nM)	18527	875.71
C_{max} (nM)	11707	3616
T_{max} (h)	0.03	3
C_{last} (nM)	10	15
T_{last} (h)	24	24
$T_{/2}$ (h)	3.8	3.2
F (%)		36

2 exhibits some selectivity (4−100-fold) for T315I Bcr-Abl (IC_{50} of 11 nM) relative to kinases such as TPR-Met, NPM-ALK, JAK-3, Flt-3. Although the cocrystal structure of **1** with Abl demonstrates binding to the inactive conformation (type-II), it is possible that an alternative binding conformation is exploited when binding to a subset of the potently inhibited kinases. Further work will be required to investigate to what extent broad inhibition of mutant alleles of Bcr-Abl can be achieved while still maintaining significant selectivity relative to other kinases. Considering that the gatekeeper residue is a crucial kinase selectivity determinant,[24] this will likely present a significant challenge. For example, a recently disclosed type-II inhibitor, imidazo[1,2-*b*]pyridazine derivative[18] currently undergoing phase I clinical trials, exhibits high potency against T315I as well as several kinases such as c-Src, Lyn, c-Kit, VEGFR2, FGFR1, and PDGFR.

In Vivo Efficacy and Toxicity of 2. To investigate whether **2** could inhibit wild-type and T315I Bcr-Abl at well tolerated doses in vivo, we investigated the tumor efficacy using a luciferase xenograft model. One shortcoming of the original **20** compound was a poor pharmacokinetic profile in mice. Compound **2** exhibited excellent pharmacokinetic parameters in mice as depicted in Table 4, with good systemic exposure (AUC = 875.71 h·nM, C_{max} = 3.6 μM) along with reasonable half-life ($t_{1/2}$ = 3.2 h) and favorable oral bioavailability

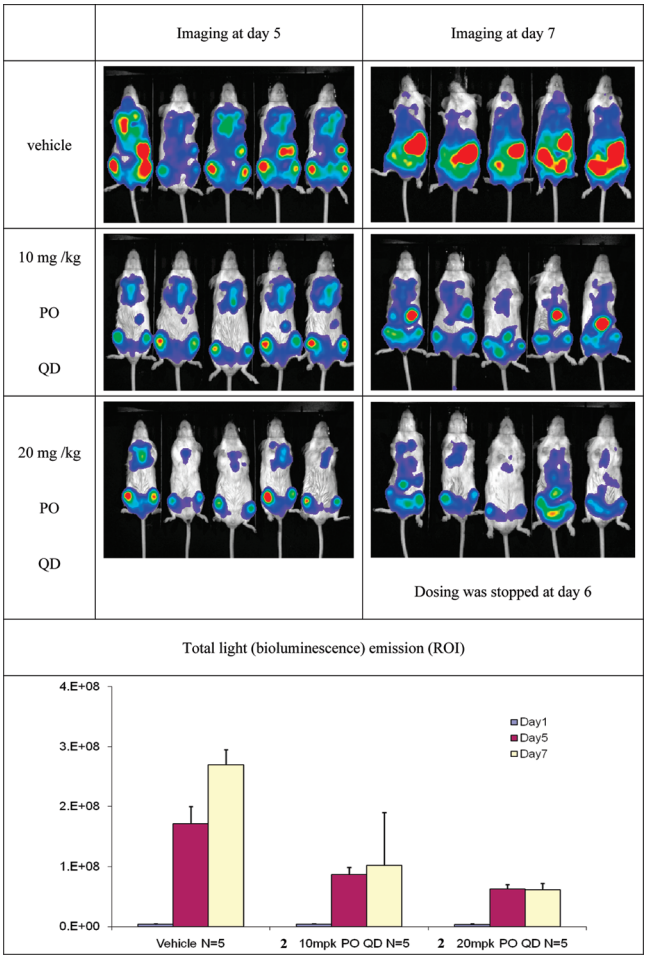

Figure 3. Bioluminescent in vivo efficacy study (oral administration, once-daily dosing) for **2** using Ba/F3-T315I-Bcr-Abl cell line that has stable luciferase expression. Mice were imaged at day 5 and 7 after **2** treatment.

(F = 36%) being observed following oral administration of a single dose of 20 mg/kg. Compound **2** displayed significant in vivo efficacy against T315I-Bcr-Abl in the bioluminescent xenograft mouse model using a transformed T315I-Bcr-Abl-Ba/F3 cell line that has stable luciferase expression. As illustrated in the Figure 3, light emission from mice that were administered an oral dose of 10 or 20 mg/kg of **2** once per day was significantly (T/C 38% and 23%, respectively) reduced compared with that from untreated control mice, indicating that **2** effectively inhibits tumor growth of T315I-Bcr-Abl-Ba/F3 cells in mice at low doses (10 mg/kg). However, appreciable (> 10%) body weight loss was observed in mice treated with doses of **2** of 20 mg/kg and above which is a common symptom of in vivo toxicity. However, the 10 mg/kg dosing group exhibited only a very small weight change as plotted in the Figure 4. The significant body weight loss in the 20 mg/kg group forced the dosing to be discontinued at day 6. An acceptable therapeutic index of **2** would be anticipated at around 10 mg/kg dose, as remarkable efficacy was observed with little body weight at this dose.

Conclusion

Our results demonstrate that it is possible to design a type-II inhibitor that can circumvent the T315I Bcr-Abl "gatekeeper" mutation by bridging the ATP and adjacent hydrophobic

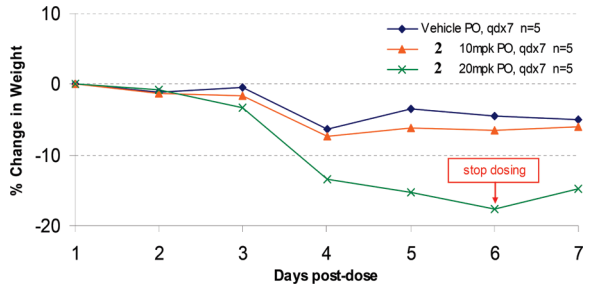

Figure 4. Mice body weight change during bioluminescent in vivo efficacy study (oral administration, once-daily dosing) for **2**.

binding site using a linker segment that can accommodate a larger gatekeeper residue. The ability of the compounds to tolerate diverse gatekeeper amino acids results in compounds with broad kinase selectivity profiles. This study also demonstrates that type-II inhibitors as a class are not necessarily more selective than type-I inhibitors. Compound **2** is likely to serve as a valuable starting point for developing type-II inhibitors for a variety of kinases of therapeutic interest.

Experimental Section

Detailed experimental procedures for Bcr-Abl kinase assay, Ba/F3 cell proliferation assay, and phosphotyrosine analysis such as autophosphorylation estimation are described in our previous publications.[19,33]

1. In Vivo Efficacy Evaluation Using T315I-Bcr-Abl-Ba/F3 Orthotopic Xenograft Model. SCID beige female mice, 6−8 weeks old (n = 5 for each **2** treated or vehicle control group), were injected via tail vein with 1×10^6 Ba/F3 cells coexpressing Bcr-abl/T315I mutant and luciferase. Three days postinjection, mice were orally dosed once daily with 10 or 20 mg/kg **2** for seven days. At day 5 and 7, bioluminescence was quantified using a Xenogen IVIS living imaging system (Caliper LifeSciences, Hopkinton, MA).

2. Experimental Section of PK Study. Male Balb/c mice, 5−6 weeks old (20−25 g), were obtained from Jackson Laboratory (Bar Harbor, ME). Compound **2** was dissolved in a 100% PEG300 solution formulation (2.5 mg/mL) and dosed at 5 mg/kg intravenously via the lateral vein (n = 3). The oral dose was prepared in a 1:1 formulation of PEG300 and distilled water and administered at 20 mg/kg via oral gavage (n = 3). Five blood samples (50 μL) were serially drawn via retro orbital sinus within 24 h after dosing. Plasma concentrations of **2** were quantified utilizing a liquid chromatography/mass spectrometry (LC/MS/MS) assay. Pharmacokinetic parameters were calculated by noncompartmental regression analysis using Winnonlin 4.0 software (Pharsight, Mountain View, CA).

3. Chemistry. Reactions were monitored by thin layer chromatography (TLC) with 0.25 mm E. Merck precoated silica gel plates (60 F254). Visualization was accomplished with either UV light, or by immersion in solutions of ninhydrin, *p*-anisaldehyde, or phosphomolybdic acid (PMA) followed by heating on a hot plate for about 10 s. Purification of reaction products was carried out by flash chromatography using Kieselgel 60 Art 9385 (230−400 mesh). The purity of all compounds was over 95% and was analyzed with Waters LCMS system (Waters 2998 photodiode array detector, Waters 3100 mass detector, Waters SFO system fluidics organizer, Waters 2545 binary gradient module, Waters Reagent Manager, Waters 2767 sample manager) using SunFireTM C18 column (4.6 mm × 50 mm, 5 μm particle size): solvent gradient = 60% (or 95%) A at 0 min, 1% A at 5 min; solvent A = 0.035% TFA in Water; solvent B = 0.035% TFA in MeOH; flow rate: 3.0 (or 2.5) mL/min. ^{1}H NMR and ^{13}C NMR spectra were obtained using a Bruker 400 MHz FT-NMR (400 MHz for ^{1}H, and 100 MHz for ^{13}C), or a Varian Inova-600 (600 MHz for ^{1}H) spectrometer. Chemical shifts are reported relative to chloroform (δ = 7.26) for ^{1}H NMR and chloroform (δ = 77.2) for ^{13}C NMR or dimethyl sulfoxide (δ = 2.50) for ^{1}H NMR and dimethyl sulfoxide (δ = 39.5) for ^{13}C NMR. Data are reported as (br = broad, s = singlet, d = doublet, t = triplet, q = quartet, m = multiplet). High resolution mass spectra were recorded on a 4.7 T IonSpec ESI-FTMS or a Micromass LCT ESI-TOF mass spectrometer.

Ethyl 4-(Methylamino)-2-(methylthio)pyrimidine-5-carboxylate (6). To a solution of compound **5** (1.0 g, 4.3 mmol) in THF (14.3 mL) was added 2.0 M methylamine solution in THF (5.37 mL, 10.7 mmol) at 0 °C, and the reaction mixture was stirred at room temperature for 1 h. The reaction mixture was partitioned between ethyl acetate (50 mL) and saturated $NaHCO_3$ (30 mL). The organic layer was washed with brine, dried over $MgSO_4$, filtered through a pad of celite, and concentrated under reduced pressure. The resulting white solid title compound (950 mg, 97% yield) was used for the next step without further purification. R_f = 0.47 (1/4 ethyl acetate/hexane). ^{1}H NMR 600 MHz ($CDCl_3$) δ 8.60 (s, 1H), 8.16 (bs, 1H), 4.32 (q, J = 7.2 Hz, J = 13.8 Hz, 2H), 3.07 (d, J = 5.4 Hz, 3H), 2.54 (s, 3H), 1.36 (t, J = 7.2 Hz, 3H). ^{1}H NMR 400 MHz (DMSO-d_6) δ 8.49 (s, 1H), 8.23 (bs, 1H), 4.26 (q, J = 7.1 Hz, J = 14.1 Hz, 2H), 2.96 (d, J = 4.8 Hz, 3H), 2.48 (s, 3H), 1.28 (t, J = 7.1 Hz, 3H). ^{13}C NMR 100 MHz (DMSO-d_6) δ 175.49, 166.22, 160.14, 158.13, 101.26. 61.01, 27.80, 14.53, 14.04. HRMS (ESI) m/z $[M + Na]^+$ calcd 250.0626, found 250.0628.

(4-(Methylamino)-2-(methylthio)pyrimidin-5-yl)methanol (7). To a solution of compound **6** (300 mg, 1.32 mmol) in THF (6.6 mL) was added 2.0 M lithium aluminum hydride solution in THF (0.79 mL, 1.58 mmol) at 0 °C. The reaction mixture was stirred at room temperature for 2 h and treated with saturated NH_4Cl solution (2 mL). After stirred at room temperature for 30 min, the reaction mixture was filtered through a pad of celite. The filtrate was partitioned between ethyl acetate (30 mL) and water (20 mL). The organic layer was washed with brine, dried over $MgSO_4$, filtered through a pad of celite, and concentrated under reduced pressure. The resulting white solid (210 mg, 86% yield) was used for the next step without further purification. R_f = 0.37 (100% ethyl acetate). ^{1}H NMR 600 MHz ($CDCl_3$) δ 7.61 (s, 1H), 5.90 (bs, 1H), 4.76 (s, 2H), 3.03 (d, J = 5.4 Hz, 3H), 2.51 (s, 3H). ^{1}H NMR 400 MHz (DMSO-d_6) δ 7.80 (s, 1H), 6.81 (bs, 1H), 5.05, (t, J = 5.4 Hz, 1H), 4.28 (d, J = 5.2 Hz, 2H), 2.84 (d, J = 4.6 Hz, 3H), 2.41 (s, 3H). ^{13}C NMR 100 MHz (DMSO-d_6) δ 169.17, 160.45, 152.04, 113.90, 57.99, 27.71, 13.79. HRMS (ESI) m/z $[M + Na]^+$ calcd 208.0521, found 208.0520.

4-(Methylamino)-2-(methylthio)pyrimidine-5-carbaldehyde (8). To a solution of compound **7** (210 mg, 1.14 mmol) in dichloromethane (3.8 mL) was added activated manganese(IV) oxide (980 mg, 11.4 mmol) at room temperature and stirred for overnight. The reaction mixture was filtered through a pad of celite and concentrated under reduced pressure. The resulting crude product was purified by flash silica gel chromatography with ethyl acetate/hexane (1/9 to 1/4) to give (190 mg, 89% yield) of the title product as a white solid. R_f = 0.29 (1/4 ethyl acetate/hexane). ^{1}H NMR 600 MHz ($CDCl_3$) δ 9.67 (s, 1H), 8.52 (bs, 1H), 8.27 (s, 1H), 3.10 (d, J = 5.4 Hz, 3H), 2.54 (s, 3H). ^{1}H NMR 400 MHz (DMSO-d_6) δ 9.75 (s, 1H), 8.62 (bs, 1H), 8.49 (s, 1H), 2.98 (d, J = 4.8 Hz, 3H), 2.49 (s, 3H). ^{13}C NMR 100 MHz (DMSO-d_6) δ 192.11, 176.34, 163.80, 158.87, 109.95, 27.57, 14.12. LCMS m/z 184.2 $[M + H]^+$.

***N*-(3-Amino-4-methylphenyl)-3-(trifluoromethyl)benzamide (9).** To a solution of 4-methyl-3-nitrobenzenamine (2.0 g, 13.15 mmol) in dried THF (65 mL) were added DIEA (3.26 mL, 19.73 mmol) and 3-(trifluoromethyl)benzoyl chloride (3.0 g, 14.46 mmol) at 0 °C. The reaction mixture stirred for 3 h at room temperature. The reaction mixture was partitioned between ethyl acetate (100 mL) and saturated $NaHCO_3$ (50 mL). The organic layer was washed with brine, dried over $MgSO_4$, filtered through a

pad of celite, and concentrated under reduced pressure. The resulting white solid, *N*-(4-methyl-3-nitrophenyl)-3-(trifluoromethyl)-benzamide (3.9 g, 91% yield) was used for the next step without further purification. R_f = 0.41 (1/4 ethyl acetate/hexane). ^{1}H NMR 400 MHz (DMSO-d_6) δ 10.75 (s, 1H), 8.51 (d, J = 1.6, 1H), 8.30 (s, 1H), 8.27 (d, J = 7.8 Hz, 1H), 8.00 (m, 2H), 7.80 (t, J = 7.7 Hz, 1H), 7.48 (d, J = 8.4 Hz, 1H), 2.48 (s, 3H). ^{13}C NMR 100 MHz (DMSO-d_6) δ 164.72, 148.90, 138.22, 135.56, 133.52, 132.37, 130.27, 129.86, 129.54, 128.95, 128.49, 125.39, 124.72, 116.14, 19.75. HRMS (ESI) m/z [M + Na]$^+$ calcd 347.0619, found 347.0621.

To a solution of *N*-(4-methyl-3-nitrophenyl)-3-(trifluoromethyl)-benzamide (3.0 g, 9.2 mmol) in methanol (40 mL) was added 10% Pd/C (300 mg). After two vacuum/H_2 cycles to replace air inside the reaction flask with hydrogen, the reaction mixture was stirred at room temperature under a hydrogen balloon for 4 h. The reaction mixture was filtered through a pad of celite and concentrated under reduced pressure. The title compound (2.4 g, 88% yield) was used for the next step without further purification. R_f = 0.14 (1/4 ethyl acetate/hexane). ^{1}H NMR 400 MHz (DMSO-d_6) δ 10.17 (s, 1H), 8.27 (s, 1H), 8.25 (d, J = 7.9 Hz, 1H), 7.91 (d, J = 7.8 Hz, 1H), 7.75 (t, J = 7.7 Hz, 1H), 7.15 (s, 1H), 6.87 (m, 2H), 4.89 (s, 2H), 2.04 (s, 3H). ^{13}C NMR 100 MHz (DMSO-d_6) δ 164.02, 147.05, 137.70, 136.62, 132.18, 130.20, 130.00, 129.75, 129.43, 128.22, 124.62, 117.67, 109.39, 106.99, 17.45. HRMS (ESI) m/z [M + H]$^+$ calcd 317.0878, found 317.0879.

***N*-(4-Methyl-3-((4-(methylamino)-2-(methylthio)pyrimidin-5-yl)-methylamino)phenyl)-3-(trifluoromethyl)benzamide (10).** To a solution of compound **8** (190 mg, 1.03 mmol) in methanol (5.2 mL) were added acetic acid (0.12 mL, 2.06 mmol), compound **9** (304 mg, 1.03 mmol), and Na(CN)BH_3 (323 mg, 5.15 mmol) at room temperature and stirred for overnight. The reaction mixture was partitioned between ethyl acetate (30 mL) and saturated $NaHCO_3$ (20 mL), and then the water layer was extracted with ethyl acetate (10 mL × 3). The combined organic layer was washed with brine, dried over $MgSO_4$, filtered through a pad of celite, and concentrated under reduced pressure. The resulting crude product was purified by silica gel chromatography with ethyl acetate/hexane (1/4 to 2/3) to give (334 mg, 63% yield) of the title product as a white solid. R_f = 0.21 (2/3 ethyl acetate/hexane). ^{1}H NMR 400 MHz ($CDCl_3$) δ 8.55 (s, 1H), 8.11 (s, 1H), 8.04 (d, J = 7.8 Hz, 1H), 7.76 (s, 1H), 7.74 (d, J = 7.8 Hz, 1H), 7.54 (t, J = 7.8 Hz, 1H), 7.23 (s, 1H), 7.02 (d, J = 8.0 Hz, 1H), 6.97 (dd, J = 1.7 Hz, J = 7.9 Hz, 1H), 5.86 (m, 1H), 3.98 (s, 2H), 3.41 (bs, 1H), 3.01 (d, J = 4.85 Hz, 3H), 2.51 (s, 3H), 2.07 (s, 3H). ^{13}C NMR 100 MHz ($CDCl_3$) δ 171.17, 164.59, 161.14, 153.43, 145.99, 137.03, 135.79, 131.22, 130.89, 130.45, 129.25, 128.18, 124.14, 120.09, 110.69, 109.33, 103.89, 43.57, 27.60, 17.11, 14.02. HRMS (ESI) m/z [M + Na]$^+$ calcd 484.1395, found 484.1398.

***N*-(4-Methyl-3-(1-methyl-7-(methylthio)-2-oxo-1,2-dihydropyrimido[4,5-*d*]pyrimidin-3(4*H*)-yl)phenyl)-3-(trifluoromethyl)benzamide (11).** To a solution of compound **10** (334 mg, 0.73 mmol) in 1,4-dioxane (3.65 mL) were added DIEA (0.36 mL, 2.19 mmol) and triphosgene (70 mg, 0.24 mmol) at 0 °C and stirred at room temperature for 1 h. The precipitate was filtered off and the filtrate was stirred at 110 °C for 3 h. The reaction mixture was cooled to room temperature and was partitioned between ethyl acetate (20 mL) and saturated $NaHCO_3$ (20 mL) solution. The organic layer was washed with brine, dried over $MgSO_4$, filtered through a pad of celite, and concentrated under reduced pressure. The resulting crude product was purified by silica gel chromatography with ethyl acetate/hexane (1/4 to 2/3) to give (230 mg, 65% yield) of the title product as a white solid. R_f = 0.25 (2/3 ethyl acetate/hexane). ^{1}H NMR 600 MHz ($CDCl_3$) δ 8.98 (s, 1H), 8.13 (s, 1H), 8.08 (d, J = 7.8 Hz, 1H), 8.03 (s, 1H), 7.73 (m, 2H), 7.56 (t, J = 7.8 Hz, 1H), 7.29 (d, J = 8.4 Hz, 1H), 7.03 (d, J = 8.4 Hz, 1H), 4.68 (d, J = 14.4 Hz, 1H), 4.42 (d, J = 14.4 Hz, 1H), 3.51 (s, 3H), 2.59 (s, 3H), 1.72 (s, 3H). ^{1}H NMR 400 MHz (DMSO-d_6) δ 10.52 (s, 1H), 8.41 (s, 1H), 8.24 (m, 2H), 7.97 (d, J = 7.6 Hz, 1H), 7.79 (m, 2H), 7.63 (dd, J = 1.9 Hz, J = 8.2 Hz, 1H), 7.31 (d, J = 6.3 Hz, 1H), 4.78 (d, J = 14.6 Hz, 1H), 4.59 (d, J = 14.6 Hz, 1H), 3.38 (s, 3H), 2.49 (s, 3H), 2.07 (s, 3H). ^{13}C NMR 100 MHz (DMSO-d_6) δ 170.34, 164.33, 156.87, 152.76, 152.23, 141.38, 138.06, 136.06, 132.29, 131.39, 131.25, 130.26, 128.66, 124.61, 120.38, 119.77, 108.31, 46.87, 28.53, 17.23, 14.07. HRMS (ESI) m/z [M + Na]$^+$ calcd 510.1187, found 510.1186.

***N*-(4-Methyl-3-(1-methyl-7-(methylsulfonyl)-2-oxo-1,2-dihydropyrimido[4,5-*d*]pyrimidin-3(4*H*)-yl)phenyl)-3-(trifluoromethyl)-benzamide (12).** To a solution of compound **11** (230 mg, 0.47 mmol) in dichloromethane (2 mL) was added *m*-chloroperbenzoic acid (245 mg, 1.42 mmol) at 0 °C. The reaction mixture was stirred for 30 min at 0 °C and then stirred for additional 3 h at room temperature. The reaction mixture was partitioned between dichloromethane (20 mL) and saturated $NaHCO_3$ (20 mL). The organic layer was washed with brine and dried over $MgSO_4$, filtered through a pad of celite, and concentrated under reduced pressure. The resulting white solid (200 mg, 81% yield) was used for the next step without further purification. R_f = 0.50 (4/1 ethyl acetate/hexane). ^{1}H NMR 600 MHz (DMSO-d_6) δ 10.52 (s, 1H), 8.57 (s, 1H), 8.28 (s, 1H), 8.24 (d, J = 8.4 Hz, 1H), 7.96 (d, J = 7.8 Hz, 1H), 7.84 (dd, J = 1.8 Hz, J = 9.6 Hz, 1H), 7.78 (t, J = 7.8 Hz, 1H), 7.62 (d, J = 8.4 Hz, 1H), 7.31 (d, J = 8.4 Hz, 1H), 4.93 (d, J = 15.6 Hz, 1H), 4.75 (d, J = 15.6 Hz, 1H), 3.39 (s, 3H), 2.47 (s, 3H), 2.12 (s, 3H). ^{1}H NMR 400 MHz ($CDCl_3$) δ 9.05 (s, 1H), 8.24 (s, 1H), 8.11 (s, 1H), 8.08 (d, J = 7.7 Hz, 1H), 7.72 (m, 2H), 7.56 (t, J = 7.7 Hz, 1H), 7.31 (d, J = 8.2 Hz, 1H), 7.02 (d, J = 8.3 Hz, 1H), 4.81 (d, J = 15.8 Hz, 1H), 4.59 (d, J = 15.8 Hz, 1H), 3.47 (s, 3H), 3.33 (s, 3H), 1.67 (s, 3H). ^{13}C NMR 100 MHz ($CDCl_3$) δ 164.90, 164.19, 158.12, 152.38, 152.31, 139.21, 137.75, 135.27, 131.39, 131.23, 130.78, 130.13, 129.21, 128.24, 127.85, 124.25, 120.88, 119.52, 114.54, 47.07, 39.03, 29.00, 16.31. HRMS (ESI) m/z [M + Na]$^+$ calcd 542.1086, found 542.1088.

***N*-(3-(7-Amino-1-methyl-2-oxo-1,2-dihydropyrimido[4,5-*d*]pyrimidin-3(4*H*)-yl)-4-methylphenyl)-3-(trifluoromethyl)benzamide (1).** To a solution of compound **12** (100 mg, 019 mmol) in 1,4-dioxane (1.0 mL) was added 2.0 M ammonia in 2-propanol (0.97 mL, 1.93 mmol). The reaction mixture was stirred for 24 h at 120 °C in sealed reaction vessel. The reaction mixture was cooled to room temperature and concentrated under reduced pressure. The crude reaction mixture was partitioned between ethyl acetate (10 mL), and the water layer was extracted with ethyl acetate (5 mL × 3). The combined organic layer was washed with brine, dried with $MgSO_4$, filtered through a pad of celite, and concentrated under reduced pressure. The resulting crude product was purified by silica gel chromatography with MeOH/CH_2Cl_2 (1/99 to 5/95) to give (68 mg, 77% yield) of the title product as a white solid. R_f = 0.27 (5/95 MeOH/CH_2Cl_2). ^{1}H NMR 400 MHz (DMSO-d_6) δ 10.52 (s, 1H), 8.29 (s, 1H), 8.26 (d, J = 7.9 Hz, 1H), 7.97 (d, J = 7.9 Hz, 1H), 7.92 (s, 1H), 7.78 (t, J = 7.8 Hz, 1H), 7.74 (d, J = 2.1 Hz, 1H), 7.64 (dd, J = 2.0 Hz, J = 8.3 Hz, 1H), 7.30 (d, J = 8.4 Hz, 1H), 6.57 (s, 2H), 4.60 (d, J = 13.8 Hz, 1H), 4.42 (d, J = 13.8 Hz, 1H), 3.23 (s, 3H), 2.07 (s, 3H). ^{13}C NMR 100 MHz (DMSO-d_6) δ 164.32, 163.22, 157.51, 153.94, 152.91, 141.80, 138.02, 136.07, 132.30, 131.38, 131.17, 130.25, 128.65, 124.61, 120.16, 119.80, 100.86, 47.08, 28.35, 17.27. HRMS (ESI) m/z [M + Na]$^+$ calcd 479.1419, found 479.1417.

***N*-(4-Methyl-3-(1-methyl-7-(6-methylpyridin-3-ylamino)-2-oxo-1,2-dihydropyrimido[4,5-*d*]pyrimidin-3(4*H*)-yl)phenyl)-3-(trifluoromethyl)benzamide (2).** To a solution of compound **12** (100 mg, 019 mmol) in 1,4-dioxane (1.0 mL) were added 6-methylpyridin-3-amine (104 mg, 0.96 mmol) and trifluoroacetic acid (73 uL, 0.96 mmol). The reaction mixture was stirred for 48 h at 120 °C. The reaction mixture was cooled to room temperature and was concentrated. The crude reaction mixture was partitioned between ethyl acetate (20 mL) and saturated $NaHCO_3$ (20 mL)

solution. The organic layer was washed with brine, dried with $MgSO_4$, filtered through a pad of celite, and concentrated under reduced pressure. The resulting crude product was purified by silica gel chromatography with $MeOH/CH_2Cl_2$ (1/99 to 5/95) to give (34 mg, 32% yield) of the title product as a white solid. R_f = 0.23 (5/95 $MeOH/CH_2Cl_2$). ^1H NMR 600 MHz (DMSO-d_6) δ 10.50 (s, 1H), 9.61 (s, 1H), 8.77 (d, J = 3.0 Hz, 1H), 8.28 (s, 1H), 8.25 (d, J = 8.4 Hz, 1H), 8.13 (s, 1H), 8.04 (dd, J = 2.4 Hz, J = 8.4 Hz, 1H), 7.95 (d, J = 7.8 Hz, 1H), 7.78 (m, 2H), 7.63 (dd, J = 1.8 Hz, J = 8.4 Hz, 1H), 7.30 (d, J = 8.4 Hz, 1H), 7.16 (d, J = 9.0 Hz, 1H), 4.69 (d, J = 13.8 Hz, 1H), 4.52 (d, J = 13.8 Hz, 1H), 3.32 (s, 3H), 2.40 (s, 3H), 2.12 (s, 3H). ^1H NMR 400 MHz ($CDCl_3$) δ 9.19 (s, 1H), 8.74 (d, J = 2.2 Hz, 1H), 8.17 (s, 1H), 8.13 (d, J = 7.7 Hz, 1H), 8.00 (dd, J = 2.3 Hz, J = 8.4 Hz, 1H), 7.94 (s, 1H), 7.74 (d, J = 7.7 Hz, 1H), 7.69 (s, 1H), 7.56 (m, 2H), 7.30 (d, J = 8.2 Hz, 1H), 7.17 (d, J = 8.4 Hz, 1H), 7.00 (d, J = 8.4 Hz, 1H), 4.64 (d, J = 14.1 Hz, 1H), 4.42 (d, J = 14.2 Hz, 1H), 3.51 (s, 3H), 2.54 (s, 3H), 1.62 (s, 3H). ^{13}C NMR 100 MHz ($CDCl_3$) δ 164.23, 159.20, 157.48, 153.49, 152.88, 152.19, 140.43, 139.91, 137.72, 135.61, 133.71, 131.38, 131.02, 130.87, 129.05, 128.06, 127.23, 124.38, 123.05, 120.72, 120.03, 102.73, 47.29, 28.73, 23.61, 16.24. HRMS (ESI) m/z $[M + Na]^+$ calcd 570.1841, found 542.1839.

***N*-(4-Methyl-3-(1-methyl-2-oxo-7-(phenylamino)-1,2-dihydropyrimido[4,5-*d*]pyrimidin-3(4*H*)-yl)phenyl)-3-(trifluoromethyl)benzamide (3).** To a solution of compound **12** (100 mg, 019 mmol) in 1,4-dioxane (0.5 mL) was added aniline (0.17 mL, 1.93 mmol). The reaction mixture was stirred for 24 h at 130 °C. The reaction mixture was cooled to room temperature and concentrated under reduced pressure. The crude reaction mixture was partitioned between ethyl acetate (10 mL), and the water layer was extracted with ethyl acetate (5 mL × 3). The combined organic layer was washed with brine, dried with $MgSO_4$, filtered through a pad of celite, and concentrated under reduced pressure. The resulting crude product was purified by silica gel chromatography with $MeOH/CH_2Cl_2$ (1/99 to 5/95) to give (72 mg, 70% yield) of the title product as a white solid. R_f = 0.30 (5/95 $MeOH/CH_2Cl_2$). ^1H NMR 400 MHz (DMSO-d_6) δ 10.53 (s, 1H), 9.56 (s, 1H), 8.30 (s, 1H), 8.21 (d, J = 7.9 Hz, 1H), 8.14 (s, 1H), 7.97 (d, J = 7.8 Hz, 1H), 7.78 (m, 4H), 7.65 (dd, J = 2.0 Hz, J = 8.3 Hz, 1H), 7.29 (m, 3H), 6.93 (t, J = 7.4 Hz, 1H), 4.71 (d, J = 14.1 Hz, 1H), 4.53 (d, J = 13.8 Hz, 1H), 3.26 (s, 3H), 2.13 (s, 3H). ^{13}C NMR 100 MHz (DMSO-d_6) δ 164.33, 159.46, 157.39, 153.65, 152.65, 141.67, 141.02, 138.06, 136.08, 132.30, 131.42, 131.22, 130.25, 128.95, 128.64, 124.62, 121.75, 120.26, 119.82, 119.25, 103.12, 47.12, 28.70, 17.27. HRMS (ESI) m/z $[M + Na]^+$ calcd 555.1732, found 555.1730.

***N*-Methyl-5-((2-methyl-5-nitrophenylamino)methyl)-2-(methylthio)pyrimidin-4-amine (14).** To a solution of compound **8** (500 mg, 2.73 mmol) in methanol (10 mL) were added acetic acid (0.31 mL, 2.06 mmol), 2-methyl-5-nitrobenzenamine (415 mg, 2.73 mmol), and $Na(CN)BH_3$ (858 mg, 13.66 mmol) at room temperature and stirred for overnight. The reaction mixture was partitioned between ethyl acetate (50 mL) and saturated $NaHCO_3$ (30 mL), and then the water layer was extracted with ethyl acetate (30 mL × 3). The combined organic layer was washed with brine, dried over $MgSO_4$, filtered through a pad of celite, and concentrated under reduced pressure. The resulting crude product was purified by silica gel chromatography with ethyl acetate/hexane (1/4 to 2/3) to give (310 mg, 36% yield) of the title product as a yellow solid. R_f = 0.30 (2/3 ethyl acetate/hexane). ^1H NMR 400 MHz (DMSO-d_6) δ 7.86 (s, 1H), 7.38 (dd, J = 2.1 Hz, J = 8.6 Hz, 1H), 7.22 (d, J = 8.2 Hz, 1H), 7.18 (d, J = 2.0 Hz, 1H), 7.14 (m, 1H), 5.98 (m, 1H), 4.18 (d, J = 5.5 Hz, 2H), 2.88 (d, J = 4.5 Hz, 3H), 2.36 (s, 3H), 2.20 (s, 3H). ^{13}C NMR 100 MHz (DMSO-d_6) δ 169.21, 160.48, 152.97, 147.41, 147.12, 131.10, 130.72, 111.25, 109.93, 103.22, 27.81, 18.41, 13.78. HRMS (ESI) m/z $[M + Na]^+$ calcd 342.1001, found 342.1003.

1-Methyl-3-(2-methyl-5-nitrophenyl)-7-(methylthio)-3,4-dihydropyrimido[4,5-*d*]pyrimidin-2(1*H*)-one (15). To a solution of compound **14** (200 mg, 0.63 mmol) in 1,4-dioxane (3.0 mL) were added DIEA (0.31 mL, 1.88 mmol) and triphosgene (65 mg, 0.22 mmol) at 0 °C and stirred at room temperature for 1 h. The precipitate was filtered off and the filtrate was stirred at 110 °C for 3 h. The reaction mixture was cooled to room temperature and was partitioned between ethyl acetate (20 mL) and saturated $NaHCO_3$ (20 mL) solution. The organic layer was washed with brine, dried over $MgSO_4$, filtered through a pad of celite, and concentrated under reduced pressure. The resulting crude product was purified by silica gel chromatography with ethyl acetate/hexane (1/4 to 2/3) to give (170 mg, 78% yield) of the title product as a yellow solid. R_f = 0.39 (2/3 ethyl acetate/hexane). ^1H NMR 400 MHz ($CDCl_3$) δ 8.16 (d, J = 2.2 Hz, 1H), 8.15 (dd, J = 2.3 Hz, J = 8.3 Hz, 1H), 8.10 (s, 1H), 7.49 (d, J = 8.3 Hz, 1H), 4.85 (d, J = 14.1 Hz, 1H), 4.52 (d, J = 14.6 Hz, 1H), 3.47 (s, 3H), 2.59 (s, 3H), 2.33 (s, 3H). ^{13}C NMR 100 MHz ($CDCl_3$) δ 172.29, 156.49, 152.38, 151.97, 147.04, 144.22, 141.34, 132.00, 122.97, 122.35, 106.31, 47.16, 28.59, 18.17, 14.23. HRMS (ESI) m/z $[M + Na]^+$ calcd 368.0793, found 368.0794.

3-(5-Amino-2-methylphenyl)-1-methyl-7-(methylthio)-3,4-dihydropyrimido[4,5-*d*]pyrimidin-2(1*H*)-one (16). To a solution of compound **15** (150 mg, 0.43 mmol) in methanol (2 mL) was added 10% Pd/C (15 mg). After two vacuum/H_2 cycles to replace air inside the reaction flask with hydrogen balloon, the reaction mixture was stirred at room temperature for 6 h. The reaction mixture was filtered through a pad of Celite and concentrated under reduced pressure. The title product (130 mg, 94% yield) was used for the next step without further purification. R_f = 0.31 (4/1 ethyl acetate/hexane). ^1H NMR 400 MHz ($CDCl_3$) δ 8.03 (s, 1H), 7.06 (d, J = 8.1 Hz, 1H), 6.62 (dd, J = 2.4 Hz, J = 8.1 Hz, 1H), 6.56 (d, J = 2.3 Hz, 1H), 4.66 (d, J = 14.6 Hz, 1H), 4.48 (d, J = 14.6 Hz, 1H), 3.44 (s, 3H), 2.57 (s, 3H), 2.09 (s, 3H). ^{13}C NMR 100 MHz ($CDCl_3$) δ 171.71, 156.82, 152.50, 151.67, 145.75, 141.05, 131.97, 124.93, 115.43, 113.56, 160.82, 47.19, 28.44, 16.64, 14.20. HRMS (ESI) m/z $[M + Na]^+$ calcd 338.1052, found 338.1055.

3-(4-Methyl-1*H*-imidazol-1-yl)-5-(trifluoromethyl)benzoic Acid (17). To a solution of 3-fluoro-5-(trifluoromethyl)benzonitrile (5.0 g, 26.45 mmol) in *N*,*N*-dimethylacetamide (25 mL) was added 4-methyl imidazole (6.5 g, 79.36 mmol). The reaction mixture was stirred at 150 °C for 24 h. The reaction mixture was cooled to room temperature. The crude reaction mixture was partitioned between ethyl acetate (100 mL), and the water layer was extracted with ethyl acetate (5 mL × 3). The combined organic layer was washed with brine, dried with $MgSO_4$, filtered through a pad of celite, and concentrated under reduced pressure. The resulting crude product was purified by silica gel chromatography with ethyl acetate/hexane (1/3 to 2/1) to give (4.8 g, 73% yield) 3-(4-methyl-1*H*-imidazol-1-yl)-5-(trifluoromethyl)benzonitrile as a white solid. R_f = 0.21 (3/2 ethyl acetate/hexane). ^1H NMR 400 MHz (DMSO-d_6) δ 8.53 (s, 1H), 8.45 (s, 1H), 8.40 (s, 1H), 8.24 (s, 1H), 7.71 (s, 1H), 2.15 (s, 3H). ^{13}C NMR 100 MHz (DMSO-d_6) δ 139.60, 138.64, 135.73, 132.38, 132.5, 127.22, 126.89, 121.07, 117.45, 114.55, 114.44, 14.00. HRMS (ESI) m/z $[M + Na]^+$ calcd 274.0568, found 274.0569.

To a solution of 3-(4-methyl-1*H*-imidazol-1-yl)-5-(trifluoromethyl)benzonitrile (3 g, 11.95 mmol) in dioxane (30 mL) was added 2 N NaOH solution (30 mL, 59.76 mmol). The reaction mixture was stirred for 24 h under reflux condition. The reaction mixture was cooled to room temperature, and the organic solvent was removed under reduced pressure. To a reaction mixture was added 6N HCl solution until white solid (pH = 4−5) precipitated. The produced white solid was filtered and dried over nitrogen gas flow. The title compound (2.6 g, 80% yield) was used for the next step without further purification. ^1H NMR 400 MHz (DMSO-d_6) δ 8.51 (s, 1H), 8.35 (s, 1H), 8.40 (s, 1H), 8.29 (s, 1H), 8.07 (s, 1H), 7.74 (s, 1H), 2.17 (s, 3H). ^{13}C NMR 100 MHz (DMSO-d_6) δ 165.81, 138.72, 138.39, 135.70, 134.41, 131.64, 131.31, 124.46, 123.59, 121.14, 115.0, 13.68. HRMS (ESI) m/z $[M + H]^+$ calcd 271.0689, found 271.0691.

3-(4-Methyl-1*H*-imidazol-1-yl)-*N*-(4-methyl-3-(1-methyl-7-(methylthio)-2-oxo-1,2-dihydropyrimido[4,5-*d*]pyrimidin-3(4*H*)-yl)phenyl)-5-(trifluoromethyl)benzamide (18). To a solution of compound **16** (100 mg, 0.32 mmol) in dried DMF (1.5 mL) were added compound **17** (86 mg, 0.32 mmol), HATU (362 mg, 0.95 mmol), and DIEA (0.26 mL, 1.58 mmol). The reaction mixture was stirred for 24 h at room temperature. The reaction mixture was partitioned between ethyl acetate (5 mL) and water (5 mL), and then the water layer was extracted with ethyl acetate (5 mL × 3). The combined organic layer was washed with brine, dried over $MgSO_4$, filtered through a pad of celite, and concentrated under reduced pressure. The resulting crude product was purified by silica gel chromatography with $MeOH/CH_2Cl_2$ (1/95 to 5/95) to give (161 mg, 89% yield) of the title product as a white solid. R_f = 0.28 (5/95 $MeOH/CH_2Cl_2$). ^{1}H NMR 400 MHz ($CDCl_3$) δ 9.47 (s, 1H), 8.14 (m, 2H), 8.04 (s, 1H), 7.88 (s, 1H), 7.71 (s, 1H), 7.60 (s, 1H), 7.39 (d, J = 7.5 Hz, 1H), 7.10 (s, 1H), 7.02 (d, J = 8.4 Hz, 1H), 4.68 (d, J = 14.7 Hz, 1H), 4.46 (d, J = 14.7 Hz, 1H), 3.47 (s, 3H), 2.59 (s, 3H), 2.28 (s, 3H), 1.68 (s, 3H). ^{13}C NMR 100 MHz ($CDCl_3$) δ 172.11, 163.03, 156.32, 153.62, 152.04, 140.61, 139.78, 138.00, 137.64, 134.47, 132.73, 132.40, 131.16, 130.89, 124.49, 123.32, 122.64, 120.85, 120.01, 119.80, 114.15, 105.34, 47.21, 28.48, 16.36, 14.22, 13.60. HRMS (ESI) m/z $[M + Na]^+$ calcd 590.1562, found 590.1563.

3-(4-Methyl-1*H*-imidazol-1-yl)-*N*-(4-methyl-3-(1-methyl-7-(methylsulfonyl)-2-oxo-1,2-dihydropyrimido[4,5-*d*]pyrimidin-3(4*H*)-yl)phenyl)-5-(trifluoromethyl)benzamide (19). To a solution of compound **18** (130 mg, 0.23 mmol) in dichloromethane (1 mL) was added *m*-chloroperbenzoic acid (158 mg, 0.91 mmol) at 0 °C. The reaction mixture was stirred for 30 min at 0 °C and then stirred for 3 h at room temperature. The reaction mixture was partitioned between dichloromethane (10 mL) and saturated $NaHCO_3$ (10 mL). The organic layer was washed with brine, dried over $MgSO_4$, filtered through a pad of celite, and concentrated under reduce pressure. The resulting white solid (122 mg, 88% yield) was used for the next step without further purification. R_f = 0.27 (5/95 $MeOH/CH_2Cl_2$). ^{1}H NMR 400 MHz (DMSO-d_6) δ 10.66 (s, 1H), 8.58 (s, 1H), 8.47 (s, 1H), 8.39 (s, 1H), 8.23 (s, 1H), 8.16 (s, 1H), 7.85 (m, 1H), 7.69 (s, 1H), 7.67 (dd, J = 1.9 Hz, J = 8.3 Hz, 1H), 7.34 (d, J = 8.4 Hz, 1H), 4.94 (d, J = 15.6 Hz, 1H), 4.77 (d, J = 15.6 Hz, 1H), 3.40 (s, 3H), 3.35 (s, 3H), 2.14 (s, 3H), 2.10 (s, 3H). ^{13}C NMR 100 MHz (DMSO-d_6) δ 164.63, 163.56, 158.19, 153.02, 151.55, 141.01, 139.42, 138.21, 137.96, 137.84, 135.72, 131.63, 131.48, 131.38, 123.06, 122.33, 120.64, 119.83, 119.63, 115.94, 114.72, 47.14, 28.95, 17.20, 14.00.HRMS (ESI) m/z $[M + Na]^+$ calcd 622.1460, found 622.1463.

3-(4-Methyl-1*H*-imidazol-1-yl)-*N*-(4-methyl-3-(1-methyl-7-(methylamino)-2-oxo-1,2-dihydropyrimido[4,5-*d*]pyrimidin-3(4*H*)-yl)-phenyl)-5-(trifluoromethyl)benzamide (4). To a solution of compound **19** (100 mg, 0.16 mmol) in 1,4-dioxane (2.0 mL) was added 2.0 M methylamine in THF (0.83 mL, 1.67 mmol). The reaction mixture was stirred for 24 h at 120 °C in the sealed reaction vessel. The reaction mixture was cooled to room temperature and concentrated under reduced pressure. The crude reaction mixture was partitioned between ethyl acetate (10 mL), and the water layer was extracted with ethyl acetate (5 mL × 3). The combined organic layer was washed with brine, dried over $MgSO_4$, filtered through a pad of celite, and concentrated under reduced pressure. The resulting crude product was purified by silica gel chromatography with $MeOH/CH_2Cl_2$ (1/99 to 5/95) to give (75 mg, 82% yield) of the title product as a white solid. R_f = 0.23 (5/95 $MeOH/CH_2Cl_2$). ^{1}H NMR 400 MHz ($CDCl_3$) 9.49 (s, 1H), 8.15 (s, 2H), 7.89 (s, 1H), 7.83 (s, 1H), 7.69 (s, 1H), 7.49 (s, 1H), 7.46 (d, J = 7.9 Hz, 1H), 7.10 (s, 1H), 6.98 (d, J = 8.4 Hz, 1H), 5.18 (m, 1H), 4.56 (d, J = 13.8 Hz, 1H), 4.35 (d, J = 13.8 Hz, 1H), 3.36 (s, 3H), 3.03 (d, J = 5.0 Hz, 3H), 2.28 (s, 3H), 1.60 (s, 3H). ^{13}C NMR 100 MHz ($CDCl_3$) δ 163.01, 162.45, 157.13, 154.23, 153.09, 140.58, 140.07, 137.94, 137.83, 137.72, 134.51, 132.64, 132.31, 131.00, 130.73, 124.53, 123.38, 122.84, 120.19, 119.66, 119.10, 114.16, 47.38, 28.44, 28.20, 16.22, 13.64. HRMS (ESI) m/z $[M + Na]^+$ calcd 573.1950, found 573.1952.

Acknowledgment. We thank Sungjoon Kim, Xiang-ju Gu for Ba/F3 cell proliferation assay, and acknowledge scientific guidance from Peter G. Schultz.

References

(1) Weisberg, E.; Manley, P. W.; Breitenstein, W.; Bruggen, J.; Cowan-Jacob, S. W.; Ray, A.; Huntly, B.; Fabbro, D.; Fendrich, G.; Hall-Meyers, E.; Kung, A. L.; Mestan, J.; Daley, G. Q.; Callahan, L.; Catley, L.; Cavazza, C.; Azam, M.; Neuberg, D.; Wright, R. D.; Gilliland, D. G.; Griffin, J. D. Characterization of AMN107, a selective inhibitor of native and mutant Bcr-Abl. *Cancer Cell* **2005**, *7* (2), 129–141.

(2) Puttini, M.; Coluccia, A. M.; Boschelli, F.; Cleris, L.; Marchesi, E.; Donella-Deana, A.; Ahmed, S.; Redaelli, S.; Piazza, R.; Magistroni, V.; Andreoni, F.; Scapozza, L.; Formelli, F.; Gambacorti-Passerini, C. In vitro and in vivo activity of SKI-606, a novel Src-Abl inhibitor, against imatinib-resistant Bcr-Abl+ neoplastic cells. *Cancer Res.* **2006**, *66* (23), 11314–11322.

(3) Shah, N. P.; Tran, C.; Lee, F. Y.; Chen, P.; Norris, D.; Sawyers, C. L. Overriding imatinib resistance with a novel ABL kinase inhibitor. *Science* **2004**, *305* (5682), 399–401.

(4) O'Hare, T.; Walters, D. K.; Deininger, M. W.; Druker, B. J. AMN107: tightening the grip of imatinib. *Cancer Cell* **2005**, *7* (2), 117–119.

(5) Miyamoto, N.; Sugita, K.; Goi, K.; Inukai, T.; Lijima, K.; Tezuka, T.; Kojika, S.; Nakamura, M.; Kagami, K.; Nakazawa, S. The JAK2 inhibitor AG490 predominantly abrogates the growth of human B-precursor leukemic cells with 11q23 translocation or Philadelphia chromosome. *Leukemia* **2001**, *15* (11), 1758–1768.

(6) Samanta, A. K.; Lin, H.; Sun, T.; Kantarjian, H.; Arlinghaus, R. B. Janus kinase 2: a critical target in chronic myelogenous leukemia. *Cancer Res.* **2006**, *66* (13), 6468–6472.

(7) Summy, J. M.; Trevino, J. G.; Lesslie, D. P.; Baker, C. H.; Shakespeare, W. C.; Wang, Y.; Sundaramoorthi, R.; Metcalf, C. A.; Keats, J. A.; Sawyer, T. K.; Gallick, G. E. AP23846, a novel and highly potent Src family kinase inhibitor, reduces vascular endothelial growth factor and interleukin-8 expression in human solid tumor cell lines and abrogates downstream angiogenic processes. *Mol. Cancer Ther.* **2005**, *4* (12), 1900–1911.

(8) Azam, M; Nardi, V.; Shakespeare, W. C.; Metcalf, C. A., III; Bohacek, R. S.; Wang, Y.; Sundaramoorthi, R.; Sliz, P.; Veach, D. R.; Bornmann, W. G.; Clarkson, B.; Dalgarno, D. C.; Sawyer, T. K.; Daley, G. Q. Activity of dual SRC-ABL inhibitors highlights the role of BCR/ABL kinase dynamics in drug resistance. *Proc. Natl. Acad. Sci. U.S.A.* **2006**, *103* (24), 9244–9249.

(9) Harrington, E. A.; Bebbington, D.; Moore, J.; Rasmussen, R. K.; Ajose-Adeogun, A. O.; Nakayama, T.; Graham, J. A.; Demur, C.; Hercend, T.; Diu-Hercend, A.; Su, M.; Golec, J. M.; Miller, K. M. VX-680, a potent and selective small-molecule inhibitor of the Aurora kinases, suppresses tumor growth in vivo. *Nature Med.* **2004**, *10* (3), 262–267.

(10) Carter, T. A.; Wodicka, L. M.; Shah, N. P.; Velasco, A. M.; Fabian, M. A.; Treiber, D. K.; Milanov, Z. V.; Atteridge, C. E.; Biggs, W. H., 3rd; Edeen, P. T.; Floyd, M.; Ford, J. M.; Grotzfeld, R. M.; Herrgard, S.; Insko, D. E.; Mehta, S. A.; Patel, H. K.; Pao, W.; Sawyers, C. L.; Varmus, H.; Zarrinkar, P. P.; Lockhart, D. J. Inhibition of drug-resistant mutants of ABL, KIT, and EGF receptor kinases. *Proc. Natl. Acad. Sci U.S.A* **2005**, *102* (31), 11011–11016.

(11) Carpinelli, P.; Ceruti, R.; Giorgini, M. L.; Cappella, P.; Gianellini, L.; Croci, V.; Degrassi, A.; Texido, G.; Rocchetti, M.; Vianello, P.; Rusconi, L.; Storici, P.; Zugnoni, P.; Arrigoni, C.; Soncini, C.; Alli, C.; Patton, V.; Marsiglio, A.; Ballinari, D.; Pesenti, E.; Fancelli, D.; Moll, J. PHA-739358, a potent inhibitor of Aurora kinases with a selective target inhibition profile relevant to cancer. *Mol. Cancer Ther.* **2007**, *6* (12), 3158–3168.

(12) Modugno, M.; Casale, E.; Soncini, C.; Rosettani, P.; Colombo, R.; Lupi, R.; Rusconi, L.; Fancelli, D.; Carpinelli, P.; Cameron, A. D.; Isacchi, A.; Moll, J. Crystal structure of the T315I Abl mutant in complex with the aurora kinases inhibitor PHA-739358. *Cancer Res.* **2007**, *67* (17), 7987–7990.

(13) Noronha, G.; Cao, J.; Chow, C. P.; Dneprovskaia, E.; Fine, R. M.; Hood, J.; Kang, X.; Klebansky, B.; Lohse, D.; Mak, C. C.; McPherson, A.; Palanki, M. S. S.; Pathak, V. P.; Renick, J.; Soll, R.; Zeng, B. Inhibitors of ABL and the ABL-T315I mutation. *Curr. Top. Med. Chem.* **2008**, *8* (10), 905–921.

(14) Gumireddy, K.; Baker, S. J.; Cosenza, S. C.; John, P.; Kang, A. D.; Robell, K. A.; Reddy, M. V.; Reddy, E. P. A non-ATP-competitive inhibitor of BCR-ABL overrides imatinib resistance. *Proc. Natl. Acad. Sci. U.S.A* **2005**, *102* (6), 1992–1997.
(15) Huang, W. S.; Zhu, X.; Wang, Y.; Azam, M.; Wen, D.; Sundaramoorthi, R.; Thomas, R. M.; Liu, S.; Banda, G.; Lentini, S. P.; Das, S.; Xu, Q.; Keats, J.; Wang, F.; Wardwell, S.; Ning, Y.; Snodgrass, J. T.; Broudy, M. I.; Russian, K.; Daley, G. Q.; Iuliucci, J.; Dalgarno, D. C.; Clackson, T.; Sawyer, T. K.; Shakespeare, W. C. 9-(Arenethenyl)purines as Dual Src/Abl Kinase Inhibitors Targeting the Inactive Conformation: Design, Synthesis, and Biological Evaluation. *J. Med. Chem.* **2009**, *52* (15), 4743–47565.
(16) Seeliger, M. A.; Ranjitkar, P.; Kasap, C.; Shan, Y.; Shaw, D. E.; Shah, N. P.; Kuriyan, J.; Maly, D. J. Equally potent inhibition of c-Src and Abl by compounds that recognize inactive kinase conformations. *Cancer Res.* **2009**, *69* (6), 2384–2392.
(17) Dar, A. C.; Lopez, M. S.; Shokat, K. M. Small molecule recognition of c-Src via the Imatinib-binding conformation. *Chem. Biol.* **2008**, *15* (10), 1015–1022.
(18) O'Hare, T.; Shakespeare, W. C.; Zhu, X.; Eide, C. A.; Rivera, V. M.; Wang, F.; Adrian, L. T.; Zhou, T.; Huang, W.-S.; Xu, Q.; Metcalf Iii, C. A.; Tyner, J. W.; Loriaux, M. M.; Corbin, A. S.; Wardwell, S.; Ning, Y.; Keats, J. A.; Wang, Y.; Sundaramoorthi, R.; Thomas, M.; Zhou, D.; Snodgrass, J.; Commodore, L.; Sawyer, T. K.; Dalgarno, D. C.; Deininger, M. W. N.; Druker, B. J.; Clackson, T. AP24534, a Pan-BCR-ABL Inhibitor for Chronic Myeloid Leukemia, Potently Inhibits the T315I Mutant and Overcomes Mutation-Based Resistance. *Cancer Cell* **2009**, *16* (5), 401–412.
(19) Okram, B.; Nagle, A.; Adrian, F. J.; Lee, C.; Ren, P.; Wang, X.; Sim, T.; Xie, Y.; Xia, G.; Spraggon, G.; Warmuth, M.; Liu, Y.; Gray, N. S. A general strategy for creating "inactive-conformation" abl inhibitors. *Chem. Biol.* **2006**, *13* (7), 779–786.
(20) Nagar, B.; Bornmann, W. G.; Pellicena, P.; Schindler, T.; Veach, D. R.; Miller, W. T.; Clarkson, B.; Kuriyan, J. Crystal structures of the kinase domain of c-Abl in complex with the small molecule inhibitors PD173955 and imatinib (STI-571). *Cancer Res.* **2002**, *62* (15), 4236–4243.
(21) Tokarski, J. S.; Newitt, J. A.; Chang, C. Y.; Cheng, J. D.; Wittekind, M.; Kiefer, S. E.; Kish, K.; Lee, F. Y.; Borzillerri, R.; Lombardo, L. J.; Xie, D.; Zhang, Y.; Klei, H. E. The structure of Dasatinib (BMS-354825) bound to activated ABL kinase domain elucidates its inhibitory activity against imatinib-resistant ABL mutants. *Cancer Res.* **2006**, *66* (11), 5790–5797.
(22) Pao, W.; Miller, V. A.; Politi, K. A.; Riely, G. J.; Somwar, R.; Zakowski, M. F.; Kris, M. G.; Varmus, H. Acquired resistance of lung adenocarcinomas to gefitinib or erlotinib is associated with a second mutation in the EGFR kinase domain. *PLoS Med.* **2005**, *2* (3), e73.
(23) Fabbro, D.; Ruetz, S.; Bodis, S.; Pruschy, M.; Csermak, K.; Man, A.; Campochiaro, P.; Wood, J.; O'Reilly, T.; Meyer, T. PKC412-a protein kinase inhibitor with a broad therapeutic potential. *Anti-Cancer Drug Des.* **2000**, *15* (1), 17–28.
(24) Cools, J.; Mentens, N.; Furet, P.; Fabbro, D.; Clark, J. J.; Griffin, J. D.; Marynen, P.; Gilliland, D. G. Prediction of resistance to small molecule FLT3 inhibitors: implications for molecularly targeted therapy of acute leukemia. *Cancer Res.* **2004**, *64* (18), 6385–6389.
(25) (a) Cools, J.; DeAngelo, D. J.; Gotlib, J.; Stover, E. H.; Legare, R. D.; Cortes, J.; Kutok, J.; Clark, J.; Galinsky, I.; Griffin, J. D.; Cross, N. C.; Tefferi, A.; Malone, J.; Alam, R.; Schrier, S. L.; Schmid, J.; Rose, M.; Vandenberghe, P.; Verhoef, G.; Boogaerts, M.; Wlodarska, I.; Kantarjian, H.; Marynen, P.; Coutre, S. E.; Stone, R.; Gilliland, D. G. A tyrosine kinase created by fusion of the PDGFRA and FIP1L1 genes as a therapeutic target of imatinib in idiopathic hypereosinophilic syndrome. *N. Engl. J. Med.* **2003**, *348* (13), 1201–1214. (b) Blencke, S.; Zech, B.; Engkvist, O.; Greff, Z.; Orfi, L.; Horvath, Z.; Keri, G.; Ullrich, A.; Daub, H. Characterization of a conserved structural determinant controlling protein kinase sensitivity to selective inhibitors. *Chem. Biol.* **2004**, *11* (5), 691–701.
(26) Kraker, A. J.; Hartl, B. G.; Amar, A. M.; Barvian, M. R.; Showalter, H. D.; Moore, C. W. Biochemical and cellular effects of c-Src kinase-selective pyrido[2,3-*d*]pyrimidine tyrosine kinase inhibitors. *Biochem. Pharmacol.* **2000**, *60* (7), 885–898.
(27) (a) Panek, R. L.; Lu, G. H.; Klutchko, S. R.; Batley, B. L.; Dahring, T. K.; Hamby, J. M.; Hallak, H.; Doherty, A. M.; Keiser, J. A. In vitro pharmacological characterization of PD 166285, a new nanomolar potent and broadly active protein tyrosine kinase inhibitor. *J. Pharmacol. Exp. Ther.* **1997**, *283* (3), 1433–1444. (b) Klutchko, S. R.; Hamby, J. M.; Boschelli, D. H.; Wu, Z.; Kraker, A. J.; Amar, A. M.; Hartl, B. G.; Shen, C.; Klohs, W. D.; Steinkampf, R. W.; Driscoll, D. L.; Nelson, J. M.; Elliott, W. L.; Roberts, B. J.; Stoner, C. L.; Vincent, P. W.; Dykes, D. J.; Panek, R. L.; Lu, G. H.; Major, T. C.; Dahring, T. K.; Hallak, H.; Bradford, L. A.; Showalter, H. D.; Doherty, A. M. 2-Substituted aminopyrido[2,3-d]pyrimidin-7(8H)-ones. Structure−activity relationships against selected tyrosine kinases and in vitro and in vivo anticancer activity. *J. Med. Chem.* **1998**, *41* (17), 3276–3292.
(28) (a) Dorsey, J. F.; Jove, R.; Kraker, A. J.; Wu, J. The pyrido[2,3-*d*]pyrimidine derivative PD180970 inhibits p210Bcr-Abl tyrosine kinase and induces apoptosis of K562 leukemic cells. *Cancer Res.* **2000**, *60* (12), 3127–3131. (b) Wisniewski, D.; Lambek, C. L.; Liu, C.; Strife, A.; Veach, D. R.; Nagar, B.; Young, M. A.; Schindler, T.; Bornmann, W. G.; Bertino, J. R.; Kuriyan, J.; Clarkson, B. Characterization of potent inhibitors of the Bcr-Abl and the c-kit receptor tyrosine kinases. *Cancer Res.* **2002**, *62* (15), 4244–4255.
(29) Cowan-Jacob, S. W.; Guez, V.; Fendrich, G.; Griffin, J. D.; Fabbro, D.; Furet, P.; Liebetanz, J.; Mestan, J.; Manley, P. W. Imatinib (STI571) resistance in chronic myelogenous leukemia: molecular basis of the underlying mechanisms and potential strategies for treatment. *Mini-Rev. Med. Chem.* **2004**, *4* (3), 285–299.
(30) (a) Melnick, J. S.; Janes, J.; Kim, S.; Chang, J. Y.; Sipes, D. G.; Gunderson, D.; Jarnes, L.; Matzen, J. T.; Garcia, M. E.; Hood, T. L.; Beigi, R.; Xia, G.; Harig, R. A.; Asatryan, H.; Yan, S. F.; Zhou, Y.; Gu, X. J.; Saadat, A.; Zhou, V.; King, F. J.; Shaw, C. M.; Su, A. I.; Downs, R.; Gray, N. S.; Schultz, P. G.; Warmuth, M.; Caldwell, J. S. An efficient rapid system for profiling the cellular activities of molecular libraries. *Proc. Natl. Acad. Sci. U.S.A* **2006**, *103* (9), 3153–3158. (b) Warmuth, M.; Kim, S.; Gu, X. J.; Xia, G.; Adrian, F. Ba/F3 cells and their use in kinase drug discovery. *Curr. Opin. Oncol.* **2007**, *19* (1), 55–60.
(31) Liu, Y.; Gray, N. S. Rational design of inhibitors that bind to inactive kinase conformations. *Nature Chem. Biol.* **2006**, *2* (7), 358–364.
(32) McDermott, U.; Sharma, S. V.; Dowell, L.; Greninger, P.; Montagut, C.; Lamb, J.; Archibald, H.; Raudales, R.; Tam, A.; Lee, D.; Rothenberg, S. M.; Supko, J. G.; Sordella, R.; Ulkus, L. E.; Iafrate, A. J.; Maheswaran, S.; Njauw, C. N.; Tsao, H.; Drew, L.; Hanke, J. H.; Ma, X.-J.; Erlander, M. G.; Gray, N. S.; Haber, D. A.; Settleman, J. Identification of genotype-correlated sensitivity to selective kinase inhibitors by using high-throughput tumor cell line profiling. *Proc. Natl. Acad. Sci. U.S.A.* **2007**, *104* (50), 19936–19941.
(33) Adrian, F. J.; Ding, Q.; Sim, T.; Velentza, A.; Sloan, C.; Liu, Y.; Zhang, G.; Hur, W.; Ding, S.; Manley, P.; Mestan, J.; Fabbro, D.; Gray, N. S. Allosteric inhibitors of Bcr-abl-dependent cell proliferation. *Nature Chem. Biol.* **2006**, *2* (2), 95–102.